Band, target, and onion patterns in $Co(OH)_2$ Liesegang systems

Layla Badr, Zeinab Moussa, Amani Hariri, and Rabih Sultan*
Department of Chemistry, American University of Beirut, P.O. Box 11-0236, Beirut 1107 2020, Lebanon
(Received 4 May 2010; revised manuscript received 4 October 2010; published 27 January 2011)

The study of morphology and shape development has gained considerable interest in certain sciences, notably biology and geology. Liesegang experiments producing $Co(OH)_2$ stratification are performed here, in one, two, and three dimensions for comparison of the pattern morphologies. We obtain well-resolved bands in one dimension, target patterns (rings) in two dimensions, and onion patterns (spherical shells) in three dimensions. The morphological characteristics of the various patterns (spacing coefficients, rate of growth of ring spacing with distance) were measured. The spacing ratio of the strata in the different spatial dimensions was found to be anticorrelated with the surface-to-volume ratio of the gel domain. Some studies featuring the importance of morphology in Liesegang systems are briefly surveyed.

DOI: 10.1103/PhysRevE.83.016109 PACS number(s): 82.40.Ck, 05.70.Ln, 05.60.Cd

I. INTRODUCTION

The importance of morphological properties in natural pattern formation [1] lies in the understanding of the various physico-chemical processes involved to produce specific shapes and the mechanism of concerted coupling between those processes. The morphology of plants [2] and bacteria colonies [3,4] and notably morphogenesis and embryonic development [5] are of central importance in biology, and ornamental features such as periodic zoning, agates, geodes, orbicules, and concretions [6] are rich manifestations of complex geophysical and geochemical dynamics.

One of the most fascinating and spectacular displays in the physical chemistry laboratory, with rich morphological structure, is the stratification of precipitate bands in a gel, the so-called Liesegang phenomenon [7–9]. This amazing self-organization feature finds its analog in a wide variety of naturally spread patterns [10]. Besides being laboratory replications of bands observed in rocks [11–15], the morphological characteristics of Liesegang patterns, along with the various geometrical laws they obey, overlap with a number of principles in mathematics and classical physics. For instance, the band locations are reminiscent of the Fibonacci series [10,16]. The band spacings in regions of different gel thicknesses obey a form of Snell's law of classical optics [17]. A brief survey of studies on morphology "engineering" in Liesegang systems is presented in the discussion in Sec. III.

Periodic precipitation patterns have characteristic empirical laws [18,19] that can sharply delineate the morphology of a given pattern. These are essentially the time law [20], band spacing law [21], band width law [19], and the so-called Matalon-Packter law [18,22–24], which relates the band spacing (coefficient)[1] to the concentrations of the inner and outer electrolytes. The latter, respectively, refer to the salt solution in the gel and the other solution (normally of notably larger concentration) laid on top of the gel, whose ions diffuse into it. The properties of Liesegang patterns were mostly studied in tubes (one-dimensional [1D] bands) and Petri dishes (two-dimensional [2D] rings); but to our knowledge, no study was carried out to correlate the two. In this paper, we prepare Liesegang patterns in one, two, and three dimensions under similar conditions and then explore and compare their morphological properties. The three-dimensional (3D) gel medium is a spherical ball of gelatin, which is prepared to be immersed in a surrounding "sea" of the outer electrolyte. Hence, diffusion of NH_4OH takes place from outside inward. As a result, the 2D experiment should be performed in an analogous way, with NH_4OH diffusing from the circular periphery toward the center of the gel medium, along a consistently radial path. This is a significant variant from the previous 2D experiments (diffusion from the center, outward). Obviously there is only *one way* to perform the 1D experiment.

Thus, in our 2D and 3D experiments, the diffusion waves and the resulting patterns propagate inward, in a way that is reminiscent of a number of observed chemical wave phenomena. Vanag and Epstein [25] reported inwardly rotating spirals in the BZ reagent system dispersed in a water-in-oil aerosol OT surfactant (AOT) microemulsion. Such structures, coined "antispirals," were obtained in different regions of the emulsion layer as the volume fraction of water droplets (ϕ_d) increased through a critical value ϕ_{cr}. Wolff *et al.* [26] discovered inward traveling target waves during CO oxidation on Pt(110). Triggered by laser-induced temperature heterogeneity pacemakers on the catalyst surface, the inward traveling waves are found over a narrow domain of parameters near low-CO partial-pressure regions. The obtained experimental results were conjectured using a complex Ginzburg-Landau equation with nonuniform frequency distribution and numerical simulations of the Krischer-Eiswirth-Ertl kinetic model [27]. Note, however, that the latter inward waves emerge from a bifurcation of specific experimental parameters, whereas our inward patterns arise from a forced reversal in the direction of the diffusion gradient.

II. EXPERIMENTAL SECTION

A. One dimension

A sample of solid cobalt chloride ($CoCl_2 \cdot 6H_2O$) (Fluka) was weighed to the nearest 0.1 mg and transferred to a beaker

*rsultan@aub.edu.lb

[1]The spacing *ratio* ρ is defined by the relation $\rho = x_{n+1}/x_n$, where x_n and x_{n+1} are the spatial locations of bands n and $n+1$ respectively. Its is established that for large n, $\rho \to 1 + p$ $(0 < p < 1)$, where p is the so-called spacing *coefficient*.

containing 25.00 ml of doubly distilled water and 2.25 g of gelatin (Difco), yielding a gel solution with $[CoCl_2 \cdot 6H_2O]_0 = 0.300$ M. The mixture was heated with constant stirring until the solution started boiling. The resulting gel was then placed in a thin glass tube (35 × 0.4 cm) sealed from one end. The gel occupied two thirds of the glass tube, and the upper edge of the gel was marked to indicate the interface between the co-precipitate solutions. The tube was allowed to stand overnight at room temperature. Then 1.33 M NH_4OH was delivered on top of the solidified cobalt chloride gel. The tube was covered with parafilm paper and allowed to stand in a thermostat chamber maintained at $T = 20 \pm 1°C$.

B. Two dimensions

A methacrylate glass Petri dish with a cover and a surrounding peripheral cavity was used. The dish has a radius of 4.4 cm (from the center to the inner edge of the cavity). The cover of 4.4 cm radius rests on tiny spacers, which impose a gel thickness of 0.7 mm. A solution of 0.300 M $CoCl_2 \cdot 6H_2O$ in gelatin (Difco, 10.0 g gelatin/100 g H_2O) was heated to boiling and homogenized by constant stirring, then poured into the Petri dish and left overnight for gelling. The next day, the gel portion at the periphery of the dish was removed without causing any distortion of the radial symmetry. The dish was then placed in the thermostat chamber at $T = 20 \pm 1°C$, for thermal equilibration. An ammonium hydroxide solution of 1.33 M concentration was delivered to fill the outer periphery around the gel, and the solution was thus allowed to diffuse radially through the gelled Co^{2+} solution. The dish was placed in the thermostat chamber and left for several days.

Immediately after the addition of the ammonia solution, a homogenous blue solid formed at the interface of the two solutions (a peripheral blue ring). A few hours later, Liesegang rings started to appear, beginning with very thin spacing, as depicted in Fig. 1.

The pattern consists of a set of concentric rings (a *target* pattern), with increasing spacing between consecutive rings as we move away from the peripheral interface, an observation consistent with the normal spacing law [21], although the diffusion takes place from outside to inside. Ring defects are seen [Fig. 1(a)], normally attributed to inhomogeneities in the layered structure of the gelatin. The constrained type of diffusion of the ammonia solution to a smaller spatial domain (from outside to inside) adds to the proneness of the system to ring breaking. Liesegang believed that ring imperfection and the rise of spiral shapes in some cases are caused by small accidental disturbances imposed on an essentially concentric ring system [28]. Similar defects have been reported in a number of 2D [29–31] Liesegang experiments. It was also pointed out that in some systems apparent Liesegang rings could actually be 2D spiral windings.

C. Three dimensions

A special cubic bloc made of methacrylate glass with a spherical cavity carved in the bloc, and a narrow channel (2.5 mm radius) connecting the cavity with the outside was carefully designed for the 3D experiment, as shown in Fig. 2(a). The inner sphere has a radius of 4.4 cm, and the cube can be

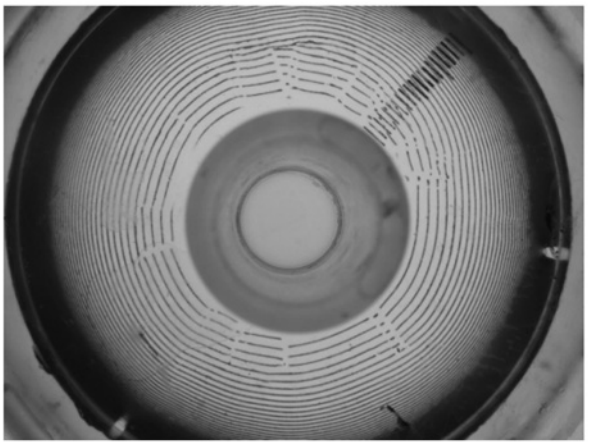

(a)

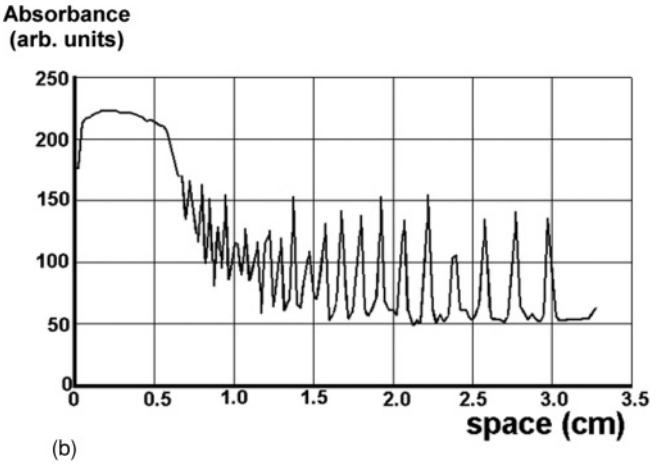

(b)

FIG. 1. (a) Target pattern of $Co(OH)_2$ Liesegang bands obtained from 1.33 M NH_4OH diffusing into a gel solution (10.0 g gelatin/100 g H_2O) containing 0.30 M Co^{2+}. (b) Map of peaks corresponding to a radial line cut across the pattern in (a). This map is used in determining the location of the rings.

opened into two halves, each bearing a hemispherical cavity. A hot solution of 0.300 M $CoCl_2 \cdot 6H_2O$ in gelatin (concentration 10.0 g gelatin/100 g H_2O) was poured through the described channel leading to the spherical cavity until the latter was totally filled. The hot gel solution filled the spherical cavity uniformly without any air bubbles. The cube was left overnight to allow the entire gel volume to solidify. The next day, the cube was further placed in the refrigerator for an additional six hours, to ensure the gelling of the central region, which was not enough exposed to achieve thermal equilibrium with the outside ambient temperature. When the solution is completely gelled, opening the box allows a perfect grabbing and retrieval of the spherical gel ball by mere scooping. The gel sphere is thus removed from the cube and completely dipped in a 1.33 M NH_4OH solution, letting the bottom of the ball rest on a circular stand fitted with a gauze canvas to allow the penetration of ammonia from the bottom, as highlighted in Fig. 2(b). The reaction setup was covered and placed in an air thermostat chamber maintained at $T = 20 \pm 1°C$ and left for several days. On the sixth day, the sphere was removed from the ammonia solution [Fig. 3(a)] and cut into two halves

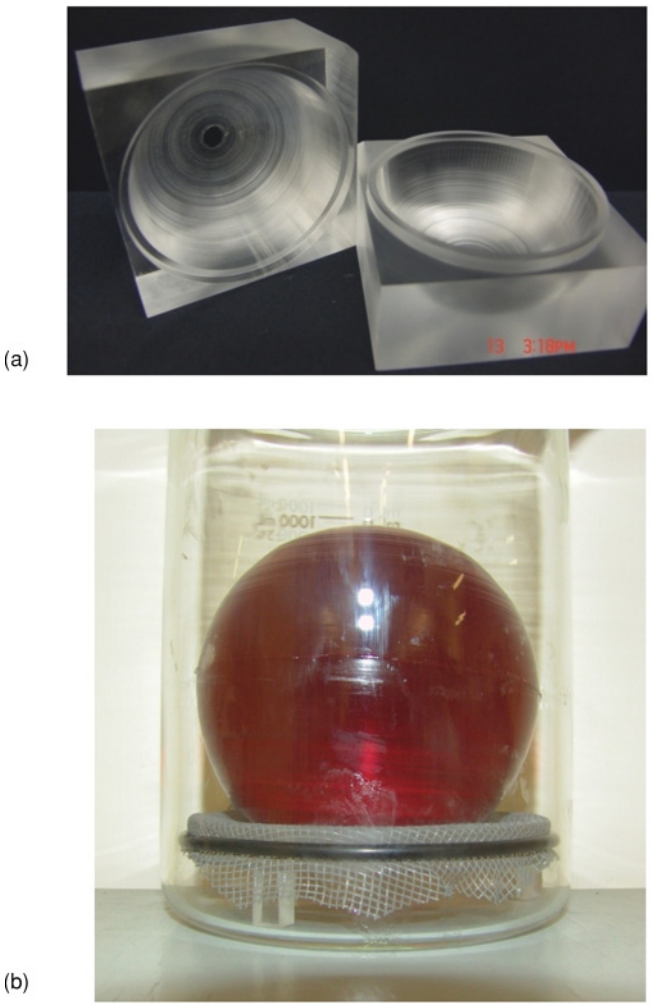

FIG. 2. (Color online) (a) Methacrylate glass cube with a spherical cavity designed especially to contain the ball of $CoCl_2$ gelatin solution. (b) The fully gelled ball before the addition of NH_4OH. Gelatin concentration: 10.0 g gelatin/100 g H_2O; 0.30 M Co^{2+}.

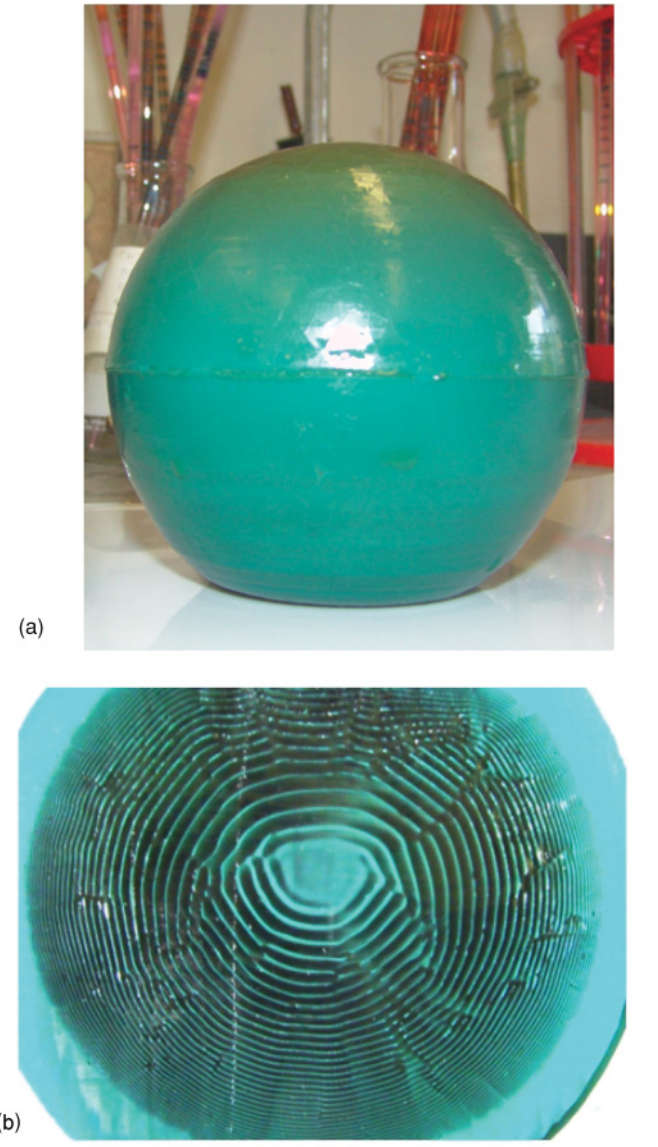

FIG. 3. (Color) (a) Same ball as in Fig. 2(b), but after immersion in 1.33 M NH_4OH, and removal after 6 days. (b) Hemisphere of the gel ball displaying an onion pattern of blue $Co(OH)_2$ rings, which are themselves cross sections of concentric spheres of precipitate.

[Fig. 3(b)]. The gel sphere in Fig. 3(b) encapsulates in it a set of concentric spheres, resembling the shells or layers in an onion. We call this outcome an *onion* pattern. Measurements of the locations of the concentric precipitate spheres from the outer edge were performed. The location of a particular shell was measured as the distance from the gel-ammonia interface (edge of the sphere ball) to the precipitate zone deposited on that spherical domain.

In the absence of redissolution by excess ammonia (achieved under the present experimental conditions [32]), the obtained Liesegang structures evolve in time via the Ostwald ripening mechanism [33,34] but remain stationary in space. By virtue of this property, Ross and his co-workers classified Liesegang structures [35,36] and other patterned precipitation phenomena [37] as time-dependent Turing [5] structures.

III. RESULTS AND DISCUSSION

To minimize the error in the measurements, a high-resolution picture of the pattern (notably 2D and 3D) was taken, and a linear cut along a radial direction was then mapped onto a graph of peaks, each indicating the location of a specific ring, relative to the interface. The locations of the 2D rings and the 3D spheres were thus determined by reading the positions of the peaks. In conformity with the general trend in Liesegang systems, the spacing between two consecutive $Co(OH)_2$ precipitate zones broadens in all three (1-, 2-, and 3D) systems, with increasing distance from the interface. This increase in spacing is the normal behavior for a Liesegang pattern [21], as opposed to a situation observed in certain systems, where the spacing becomes narrower with increasing distance, the so-called "revert spacing" case. Revert spacing was explained by special effects, peculiar to certain salt or gel systems [37–39]. The interband spacing (Δx) for each of the three dimensions was measured and plotted versus distance (x)

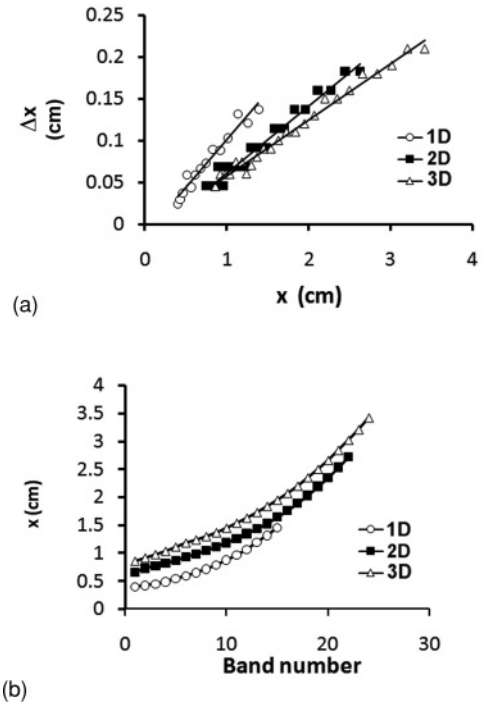

FIG. 4. (a) Variation of the band spacing Δx with distance from the NH_4OH/gel junction (x) for the 1D, 2D, and 3D experiments. (b) Variation of the band location x, with band number. In both frames, open circles: 1D; squares: 2D; open triangles: 3D.

from the point of contact of the two electrolytes at the periphery (recall here that the diffusion takes place from outside, inward). The distance x is calculated as the average location of the two bands for which the spacing is being measured. The plots are shown in Fig. 4(a). A clear trend is discerned as we go from one dimension to the next. From the relative locations of the curves in Fig. 4(a), we can conclude that the spacing at a specific location from the interface essentially decreases as we go from one to two to three dimensions. Furthermore, the slope of the plots shows a clear decreasing trend (see values in Table I). This reveals that the rate of increase of band spacing with distance decreases as we go from one to two to three dimensions. The morphological parameters characterizing each of the obtained patterns are recorded in Table I.

The average spacing ratio ρ_{ave} (the spacing ratio $\rho = x_{n+1}/x_n$, averaged over all the bands 1 to n) was found to be anticorrelated with the relative contact area between the two electrolytes. The same applies to the slope of the Δx versus x plots. The absolute contact area (called S) is the internal circular cross section of the tube in one dimension, the thin cylindrical lateral surface in two dimensions (of height $h = 0.7$ mm), and the spherical surface in three dimensions. The relative contact area, S_{rel}, is defined as the ratio of the absolute contact area (S) to the volume of the gel domain (V). Thus, $S_{\text{rel}} = S/V$.

The relative contact area (S_{rel}) increases as we go from one to two and then to three dimensions. Note that a higher S_{rel} results in both a relatively larger amount of diffused electrolyte per unit time, and a smaller spatial diffusion span, hence a larger NH_4OH concentration at a given spatial point away from the interface. Thus, at higher S_{rel}, supersaturation ($\sigma = [Co^{2+}][OH^-]^2 > \sigma_{\text{crit}}$) and nucleation are fulfilled earlier, causing the band of precipitate to form relatively closer to the interface and hence yielding a smaller spacing coefficient. This behavior is consistent with the general trend observed with high concentrations of NH_4OH, wherein smaller spacing coefficients are obtained [32]. Note further that the flow of material diffused JS (where J is the flux and S the surface area of the source) increases with distance in 2D, and more markedly in 3D, because the source diffusional area S increases as we go to higher spatial dimension. Note that a 0.500-cm increment in the diffusion length increases the source diffusional area by 0 cm^2 in a 1D tube, to 0.220 cm^2 ($2\pi\ \Delta r\ h$) in a 2D one, to 15.7 cm^2 [$4\pi\ (r_1^2 - r_2^2)$] in a 3D one, at an average distance of 1.25 cm. It thus seems that the increase in the source area overcomes the effect of the decreasing gradient, which points out the important effect of geometry on the morphological characteristics of Liesegang patterns. In other words, the gradient decreases with distance, but the decrease is less pronounced in three dimensions than two than one. This overall material increase is also responsible for the increase in the number of bands formed (16 to 22 to 24) and the decrease in the spacing coefficient (1.101 to 1.071 to 1.062) as we go from one to two to three dimensions (see Table I). Figure 4(b) shows the variation of the band location with band number in all three spatial dimensions. We clearly see that the pattern span is largest in three dimensions and smallest in one.

The plot in Fig. 5 highlights the variation of both the average spacing ratio ρ_{ave} and the slope of the Δx versus x lines with S_{rel} (the surface-to-volume ratio). Both quantities are seen to anticorrelate with S_{rel} (in one, two, and three dimensions). This is also reflected in the correlation between S_{rel} and the number of bands, which increases from 16 to 22 to 24 as we go from one to two to three dimensions (see Table I).

Interest in the detailed morphological features of Liesegang patterns has notably increased in the last decade. A suitable choice of the experimental conditions allows the engineering of predesigned morphologies and the steering of well-controlled modifications of the obtained shapes and patterns. The concentrations of the inner and outer electrolytes have a

TABLE I. Spacing ratios and slopes of the lines in Fig. 4(a) for the 1D, 2D, and 3D patterns. 1D: Cross-sectional diameter = 0.4 cm, gel height = 23.0 cm; 2D: radius $r = 4.4$ cm, gel thickness $h = 0.7$ mm; 3D: radius $r = 4.4$ cm.

Experiment	No. of bands	ρ_{ave}	Slope	S (cm^2)	V (cm^3)	S_{rel} (cm^{-1})
1D	16	1.101	0.114	0.126	2.89	0.0436
2D	22	1.071	0.079	1.94	4.26	0.455
3D	24	1.062	0.067	243	357	0.681

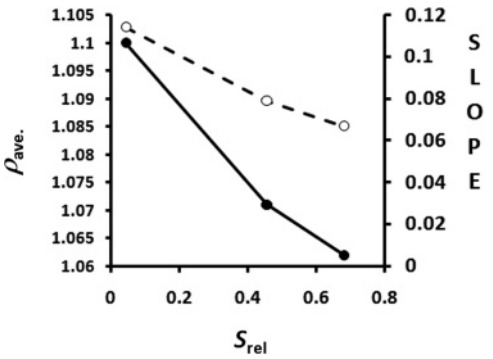

FIG. 5. Variation of the average spacing ratio, ρ_{ave}(dashed line and open circles) and the slope (solid line and black circles) of the Δx versus x lines [Fig. 4(a)], with S_{rel}, the surface-to-volume ratio.

significant impact on the band width and the band spacing. The latter generally increase with increasing inner and decreasing outer concentrations [22,32,40]. The concentration [32] and thickness [17] of the gel material have also proved a determining role. The choice of such conditions is crucial in steering the present experiments in the good direction. Band spacings in one and two dimensions have been altered and controlled by applying direct electric fields [32,41]. A diffusing electrolyte with a weak degree of dissociation (e.g., NH_4OH as opposed to NaOH) improves the interband spacing [42], whereas strong electrolytes produce very close bands. In our experiments, attempts shall be made to further improve (increase) the ring spacing for a better resolution. However, at this stage, it is important to use raw conditions without external parameters such as an electric field or pH effects to demonstrate the intrinsic character of the altered morphology. Badr and Sultan [43] devised a method for controlling the count of $Co(OH)_2$ bands to a predefined number by merely adjusting the pH of the diffusing solution (NH_4OH). The addition of acid to the invading electrolyte disturbs the stoichiometric balance between NH_4^+ and OH^- and hence favors redissolution of $Co(OH)_2$ bands over precipitation. The gradual redissolution of bands with decrease in pH subsequently enables a cut in the number of bands to a predesired value, with an increase in the interband spacing. This is a better tool to be used in our experiments and rather easy to control, because applying an electric field is difficult to realize in the 3D ball, wherein it is impossible to place an electrode at the center without disrupting the texture of the gel medium.

Liesegang rings in 2D were engineered from the assembly of functionalized, oppositely charged nanoparticles [44]. The precipitation was shown to be controlled by the condition of charge neutrality of the self-assembled monolayers rather than by the solubility product. In such systems, the spacing coefficient decreased with increasing concentration of either the inner or outer electrolyte. The design of Liesegang patterns with preassigned band locations was made possible through the use of predesigned, time-dependent electric currents [45]. Bena *et al.* [45] showed that a Liesegang pattern with controlled wavelength d, such that $x_n = dn$ could be obtained, by switching on the forward current at times $t_n = (2n)^2\tau/2$, where $\tau = d^2/2D_f$ (D_f is the diffusion coefficient controlling the diffusion front). A notable control over the curvature of Liesegang rings in two dimensions was achieved in gel media of variable thickness [17] and in circular systems subjected to the effect of a linear electric field [32]. An increase in curvature was demonstrated as the rings propagate from a thin gel film into a thicker one, and a decrease when propagation takes place from a thick gel into a thinner one [17]. The incident and refracted rings were shown to obey Snell's law of classical optics, with the indices of refraction replaced by the inverse of the spacing coefficients [17]. Shreif *et al.* [32] obtained distortions of circular symmetry into a set of parabolic rings, as a linear electric field is applied across a radial diffusion Liesegang system. The parabolas fission the original circular rings into two halves, leaving small broken arcs on both sides, and develop along an axis collinear with the field vector [32]. A variety of patterns with different dislocations was obtained [46] in 2D $Ag_2Cr_2O_7$ Liesegang systems with polygonal boundaries between the inner and outer electrolytes. Two lines of dislocations were shown to emerge from each vertex of a triangular boundary. Whereas double-armed spirals are observed with pentagonal interfaces, hexagonal boundaries were shown to restore the formation of regular concentric precipitate rings.

Additional efforts could be made to improve the band spacing, in order to perform better measurements. The selection of other Liesegang systems known to give better spacings is one possibility, but in many cases this advantage is blurred by significant ring defects and distortions. The 1D-2D-3D study could be extended to cases where electric field and pH effects are applied. This study is under present consideration.

IV. SUMMARY AND CONCLUSIONS

The main results of the present paper may now be summarized as follows:

(1) A new 3D $Co(OH)_2$ Liesegang pattern was prepared: a ball with concentric spherical shells of blue precipitate.

(2) Liesegang patterns in two and three dimensions were prepared for comparison, with diffusion of the outer electrolyte (NH_4OH) from outside inward, into the Co^{2+} gel.

(3) The span of the pattern in *number of bands* is larger in three dimensions than two than one, when prepared under exactly the same conditions.

(4) The spacing ratio decreases as we go from one to two to three dimensions.

(5) The variation of spacing with distance becomes less pronounced as we go from one to two to three dimensions.

(6) Means of improving the experiments to obtain more resolved bands were discussed in light of supporting literature information from past work.

(7) The spacing ratio in the different spatial dimensions was found to be anticorrelated with the surface-to-volume ratio of the gel domain.

ACKNOWLEDGMENTS

This work was supported by a University Research Board (URB) grant, American University of Beirut. We thank Tony Karam for his help in testing the reproducibility of some experiments.

[1] P. Ball, *Nature's Patterns: A Tapestry in Three Parts, Part 1:Shapes* (Oxford University Press, New York, 2009).
[2] R. Sattler and R. Rutishauser, Ann. Botany **80**, 571 (1997).
[3] J. A. Shapiro and M. Dworkin, eds., *Bacteria as Multicellular Organisms* (Oxford University Press, New York, 1997).
[4] V. V. Kravchenko, A. B. Medvinskii, A. N. Reshetilov, and G. R. Ivanitskii, Dokl. Akad. Nauk **364**, 114 (1999); **364**, 687 (1999).
[5] A. M. Turing, Phil. Trans. R. Soc. B **237**, 37 (1952).
[6] P. Ortoleva, Y. Chen, and W. Chen, in *Fractals and Dynamic Systems in Geoscience*, edited by J. H. Kruhl (Springer, Berlin, 1994).
[7] R. E. Liesegang, Chem. Fernwirkung. Lieseg. Photograph. Arch. **37**, 305 (1896); **37**, 331 (1914); Z. Phys. Chem. **88**, 1 (1914).
[8] H. K. Henisch, *Crystals in Gels and Liesegang Rings* (Cambridge University Press, Cambridge, UK, 1988).
[9] K. H. Stern, *A Bibliography of Liesegang Rings*, 2nd Ed. (Government Printing Office, Washington DC, 1967).
[10] S. Sadek and R. Sultan, in *Precipitation Patterns in Reaction-Diffusion Systems*, edited by I. Lagzi (Research SignPost Publications, S. Pandalai, Kerala, in press), Chapter 1.
[11] P. Ortoleva, *Geochemical Self-organization* (Oxford University Press, New York, 1994).
[12] J. H. Kruhl, ed., *Fractals and Dynamic Systems in Geoscience* (Springer, Berlin, 1994).
[13] A. E. Boudreau, Mineral. Petrol. **54**, 55 (1995).
[14] R. McBirney and R. M. Noyes, J. Petrol. **20**, 487 (1979).
[15] For a comprehensive review of banding in geochemical systems, see Ref. [10].
[16] M. Stoneham, Rep. Prog. Phys. **70**, 1055 (2007).
[17] M. Fiałkowski, A. Bitner, and B. A. Grzybowski, Phys. Rev. Lett. **94**, 018303 (2005).
[18] T. Antal, M. Droz, J. Magnin, Z. Rácz, and M. Zrinyi, J. Chem. Phys. **109**, 9479 (1998).
[19] M. Droz, J. Magnin, and M. Zrinyi, J. Chem. Phys. **110**, 9618 (1999).
[20] H. W. Morse and G. W. Pierce, Z. Physikal. Chem. **45**, 589 (1903).
[21] C. K. Jablczynski, Bull. Soc. Chim. Fr. **11**, 1592 (1923).
[22] R. Matalon and A. Packter, J. Colloid. Sci. **10**, 46 (1955).
[23] A. Packter, Kolloidn. Zh. **142**, 109 (1955).
[24] F. Zaknoun, T. Mokalled, A. Hariri, and R. Sultan, in *Precipitation Patterns in Reaction-Diffusion Systems*, edited by I. Lagzi (Research SignPost Publications, S. Pandalai, Kerala, in press), Chapter 10.
[25] V. K. Vanag and I. R. Epstein, Science **294**, 835 (2001).
[26] J. Wolff, M. Stich, C. Beta, and H. H. Rotermund, J. Phys. Chem. B **108**, 14282 (2004).
[27] K. Krischer, M. Eiswirth, and G. Ertl, J. Chem. Phys. **96**, 9161 (1992).
[28] R. E. Liesegang, Kolloidn. Zh. **87**, 57 (1939).
[29] N. R. Dhar and A. C. Chatterji, Kolloidn. Zh. **37**, 2 (1925); **37**, 89 (1925).
[30] S. C. Müller, S. Kai, and J. Ross, Science **216**, 635 (1982).
[31] H.-J. Krug and H. Brandstädter, J. Phys. Chem. A **103**, 7811 (1999).
[32] Z. Shreif, L. Mandalian, A. Abi-Haydar, and R. Sultan, Phys. Chem. Chem. Phys. **6**, 3461 (2004).
[33] W. Ostwald, Z. Phys. Chem **34**, 495 (1900).
[34] I. M. Lifshitz, and V. V. Slyozov, J. Phys. Chem. Solids **19**, 35 (1961).
[35] J. Ross, A. P. Arkin, and S. C. Müller, J. Phys. Chem. **99**, 10417 (1995).
[36] S. C. Müller and J. Ross, J. Phys. Chem. A **107**, 7997 (2003).
[37] M. Flicker and J. Ross, J. Chem. Phys. **60**, 3458 (1974).
[38] N. Kanniah, F. D. Gnanam, P. Ramasamy, and G. S. Laddha, J. Coll. Interf. Sci **80**, 369 (1981).
[39] N. Kanniah, F. D. Gnanam, and P. Ramasamy, Proc. Indian Acad. Sci. (Chem. Sci.) **93**, 801 (1984).
[40] R. Sultan and S. Sadek, J. Phys. Chem. **100**, 16912 (1996).
[41] R. Sultan and R. Halabieh, Chem. Phys. Lett. **332**, 331 (2000).
[42] B. Chopard, M. Droz, J. Magnin, Z. Rácz, and M. Zrinyi, J. Phys. Chem. A **103**, 1432 (1999).
[43] L. Badr and R. Sultan, J. Phys. Chem. A **113**, 6581 (2009).
[44] I. Lagzi, B. Kowlaczyk, and B. A. Grzybowski, J. Am. Chem. Soc. **132**, 58 (2010).
[45] I. Bena, M. Droz, I. Lagzi, K. Martens, Z. Rácz, and A. Volford, Phys. Rev. Lett. **101**, 075701 (2008).
[46] C. Pan, Q. Gao, J. Xie, and I. R. Epstein, Phys. Chem. Chem. Phys. **11**, 11033 (2009).